ORIGINAL ARTICLE

Involvement of interstitial cells of Cajal in experimental severe acute pancreatitis in rats

Liang-Liang Shi, Ming-Dong Liu, Min Chen, Xiao-Ping Zou

Liang-Liang Shi, Ming-Dong Liu, Min Chen, Xiao-Ping Zou, Department of Gastroenterology, Medical School, the Affiliated Drum Tower Hospital of Nanjing University, Nanjing 210008, Jiangsu Province, China
Author contributions: Liu MD and Zou XP contributed equally to this work; Shi LL, Liu MD and Chen M designed and performed the research; Chen M provided analytical tools and was also involved in editing the manuscript; Shi LL analyzed the data, as well as writing the paper.
Correspondence to: Xiao-Ping Zou, MD, Professor, Department of Gastroenterology, Medical School, the Affiliated Drum Tower Hospital of Nanjing University, Nanjing 210008, Jiangsu Province, China. 13770771661@163.com
Telephone: +86-25-83105206 Fax: +86-25-83105206

Abstract

AIM: To observe the changes in interstitial cells of Cajal (ICC) in rats with experimental severe acute pancreatitis (SAP).

METHODS: A total of twenty-four SD rats were randomly divided into two groups (n = 12), namely the sham (S) group and the SAP group; the SAP rat model was established by retrograde injection of 5% sodium taurocholate (1.0 mL/kg) into the pancreatic duct. Twenty-four hours later intestinal motility was assessed by testing small intestinal propulsion rate, and then the rats were sacrificed. The pancreas and jejunum were resected and underwent routine pathologic examination. Immunohistochemical staining was used to detect c-kit-positive cells in the jejunum. Expression of c-kit mRNA was detected by real-time polymerase chain reaction, and the expression of c-kit protein was evaluated by Western blotting. Ultrastructure of ICC was evaluated by transmission electron microscopy.

RESULTS: There was bleeding, necrosis and a large amount of inflammatory cell infiltration in pancreatic tissue in the SAP group, while in jejunal tissue we observed a markedly denuded mucosal layer, loss of villous tissue and a slightly dilated muscular layer. The small intestinal propulsion rate was 68.66% ± 2.66% in the S group and 41.55% ± 3.85% in the SAP group. Compared with the S group, the rate of the SAP group decreased sharply. The density of c-kit-positive cells in the SAP group was significantly lower than in the S group; the respective mean densities were 88.47 ± 10.49 in the S group and 56.11 ± 7.09 in the SAP group. The levels of c-kit protein and mRNA were 0.36 ± 0.04 and 1.29 ± 0.91 in the SAP group, respectively, which were significantly lower than those in the S group (0.53 ± 0.06, 0.64 ± 0.33, respectively). In the SAP group, ICC profiles showed the same change tendency, such as vacuolation of mitochondria, irregular vacuoles and loosened desmosome-like junctions.

CONCLUSION: Decreased c-kit-positive cells and ultrastructural changes in ICC resulting from blockade of the c-kit signaling pathway are involved in the intestinal dysmotility associated with SAP.

INTRODUCTION

In 1893, the Spanish neuro-histologist, Cajal, discovered

interstitial cells of Cajal (ICC) within the gastrointestinal wall. Since then, especially in the most recent two decades, a number of studies have established the roles of ICC in normal functions of the gastrointestinal wall primarily in 4 major groups: ICC in the submuscular plexus; ICC within the circular and longitudinal layers of muscle; ICC in the myenteric plexus (ICC-MY, also called ICC-MP); ICC in the deep muscular plexus. These cells function as pacemaker cells in the gastrointestinal wall to generate slow waves that spread from ICC to smooth muscle cells for triggering calcium entry, as a result of depolarization, and contraction as a basis for peristalsis and segmentation. They maintain normal neurotransmission and regulate mechanical activities in the gastrointestinal tract[1-5]. More recently, the discovery of c-kit along with its endogenous ligand, stem cell factor (SCF), have dramatically advanced ICC investigations in this field[6,7]. Presentation of SCF increases expression of c-kit immunoreactive ICC in culture while loss-of-function mutations of the c-kit gene cause deficiency of ICC; these have shown that the SCF/c-kit signal pathway is essential for the maintenance of ICC[8-11]. Imatinib, a novel and potent inhibitor of c-kit, abolished the spontaneous movements in circular muscles of the mouse small intestine[12], and this result suggests that the c-kit signaling of ICC plays an essential role in the spontaneous mechanical activity of intestine. Disorders of ICC may result in gastrointestinal motility dysfunctions, which lead to a number of gastrointestinal diseases, including severe acute pancreatitis (SAP). Furthermore, investigators have found that damage of ICC occurred in the muscular layer of the small intestine in experimental acute pancreatitis[13].

Despite the association of SAP with gastrointestinal motility disturbances on the basis of evidence acquired through both observational clinical[14] and experimental investigations[15,16], the detailed mechanisms of the changes in gastrointestinal motility in SAP have not been clearly elucidated. Thus, we hypothesized that ICC might play an important role in the pathogenesis of gastrointestinal dysmotility in SAP. In the present study we tested our hypothesis in a rat model of SAP.

MATERIALS AND METHODS

Animal model establishment

Twenty-four adult male Sprague-Dawley (SD) rats with body weight between 200 g and 250 g were purchased from the animal research center of the affiliated Drum Tower Hospital of Nanjing University Medical School and randomly divided into two groups of equal number (n = 12 each): the sham (S) group and the severe acute pancreatitis (SAP) group. To establish the SAP rat model, freshly prepared 5% sodium taurocholate solution was injected at a volume of 1.0 mL/kg from the duodenal papilla into the pancreatic duct. In the S group, the duodenum and pancreas of animals were manually manipulated a few times after laparotomy. All procedures took place under sterile conditions and all animals were housed under pathogen-free conditions in the animal facility with a 12-h light/dark cycle and free access to food and water. The study protocol was approved by the Medical Ethics Committee of the Hospital.

Assessment of small intestinal propulsion rate

Twenty-three hours after the operative procedure for the establishment of the SAP animal model, gastric gavage with 1 mL of methylene blue solution was performed in both groups. One hour later, the rats were euthanized *via* CO_2 asphyxiation and the small intestine in each rat was removed from the abdominal cavity. All the mesentery tissues were stripped and the total length of the small intestine from the pyloric sphincter of the distal stomach to the distal end of the ileum was measured. The movement of the methylene blue solution in the small intestine was observed and recorded. The small intestinal propulsion rate was calculated as the product of the distance of the methylene blue traveled within 30 min immediate after the removal of the small intestine divided by the total length of the small intestine.

Histopathologic examination of the pancreas and the jejunum

Both the pancreas and the jejunum were removed at the time of harvest of the small intestine described above. Four segments of the jejunum 15 cm distal to the ligament of Truiz, approximately 10 mm each in length, were collected for the following study. One segment of the jejunum was opened, cleaned, and inspected macroscopically along with the pancreas that was transversely sectioned, for visible pathologic changes. After gross examination, both organs were fixed with 10% buffered neutral formalin solution for 24 h. The tissue from both organs was sectioned at 4 μm in thickness. Histology sections were stained with hematoxylin and eosin and evaluated microscopically by experienced pathologists.

Real-time polymerase chain reaction

In the jejunal tissue freshly harvested previously, total RNA was isolated from the jejunum segments with mucosa stripped using TRIzol® reagent following the manufacturer's instructions. The reverse transcription (RT) was performed in a 20 μL reaction mixture containing 1 μg total RNA by using a PrimeScript RT Reagent Kit (Perfect Real Time, Takara Bio Inc., Otsu, Japan) according to the manufacturer's protocol. The RT reaction product was amplified by using the SYBR Premix Ex Taq (Takara Bio Inc., Otsu, Japan) and ABI PRISM 7500 Real-time PCR system according to the manufacturer's protocol. Primers of c-kit were as follows: 5'-TGGATCAGCAAATGTCA-CAACAAC-3' (forward) and 5'-TAGGCCTCGAACT-CAACAACCA-3' (reverse). The predicted size of the c-kit-PCR product was 132 bp. The primers of β-actin were: 5'-TCGTGCGTGACATTAAAGAG-3' (forward) and 5'-ATTGCCGATAGTGATGACCT-3' (reverse). The predicted size of the β actin-PCR product was 134 bp. Mean fold changes for each sample were calculated

by using the $2^{-\Delta\Delta Ct}$ method as previously described[17].

Immunohistochemical staining

The segments of jejunum harvested previously were immersed in a fixative containing 4% paraformaldehyde for 6 h at 4 ℃. Then the segments were embedded with the optimum cutting temperature compound and sectioned at 10 μm in thickness. The tissue section was mounted on glass slides. For the c-kit staining, tissue sections were incubated with 0.3% Triton X in 10% normal rabbit serum for 60 min and then incubated with the goat anti-c-kit polyclonal antibody (clone sc-1494; Santa Cruz Biotechnology, Inc., Santa Cruz, CA, United States) at 4 ℃ overnight. Next, we applied a biotin-free polymeric horseradish peroxidase (HRP)-linked antibody conjugate system for 20 min followed by DAB condensed chromogen for 5 min. Tissue sections were counterstained with hematoxylin and eosin (HE). For negative control experiments, the primary antibody was omitted. Images of c-kit-positive cells were taken in 4 randomly chosen fields (× 200 magnification) per tissue section. The positive cell density was assessed with the Image-Pro Plus 6.0 software (Media Cybernetics, Bethesda, MD, United States).

Western blotting

A segment of the jejunum was cut along the mesenteric axis and stripped of the mucosa. The remaining jejunal tissue was immediately snap-frozen in liquid nitrogen and stored at -80 ℃. After homogenization in extraction buffer (50 mmol/L Tris-Cl (pH 7.5), 150 mmol/L NaCl, 1% Triton X-100, and 1 mmol/L PMSF), the lysate was collected and centrifuged at 4 ℃ for 15 min at 10 000 r/min to remove the insoluble material. The protein concentration of the supernatant was measured by spectrophotometry using the BCA protein assay method (Pierce, Rockford, IL, United States). The samples were electrophoresed on a 10% SDS-polyacrylamide gel, and transferred to a PVDF transfer membrane (Millipore, Bedford, MA, United States). The membrane was then incubated with 5% skimmed cow's milk overnight at 4 ℃ to block nonspecific binding sites and then incubated with the primary c-kit antibody (clone sc-1494; Santa Cruz Biotechnology, Inc., Santa Cruz, CA, United States) applied for 1 h at room temperature. After washing, the secondary matching peroxidase-conjugated antibody was applied to the membrane and incubated for 1 h at room temperature. Specific protein bands were visualized with an X-ray film using the chemiluminescence detection kit (ECL Western blotting detection; Millipore Corp). Optical density of the bands was analyzed with software Quantity One.

Electron microscopy

Immediately after resection, blocks of jejunal tissue were cut and immersed into a fixative containing 5% glutaraldehyde and stored at 20 ℃ for at least 2 h. Following fixation, tissues were cut into small pieces (1 mm × 2 mm) and further fixed in 5% glutaraldehyde overnight, and then rinsed for 60 min in 0.1 mol/L phosphate buffer, pH 7.3, and postfixed in 2% OsO₄ in 0.1 mol/L phosphate buffer for 2 h. The tissue specimens were subsequently dehydrated and embedded. Thin sections were cut at 1 μm in thickness and stained with toluidine blue for light microscopy to select suitable areas for ultrathin sectioning. Ultrathin sections were cut at 70-80 nm, mounted onto copper grids, and stained with lead citrate for electron microscopy with a Philips Morgagni 261 EM microscope.

Statistical analysis

The data obtained were expressed as mean ± SD. Comparison between the two groups was performed by using the Student t-test, and the differences with $P < 0.05$ were considered as statistically significant. All data were analyzed with SPSS 13.0 software (SPSS Inc., Chicago, IL, United States).

RESULTS

Small intestinal propulsion rate

The small intestinal propulsion rate was significantly lower in the SAP group than in the S group. The respective rate was 68.66% ± 2.66% in the S group and 41.55% ± 3.85% in the SAP group.

Pathological changes

Under gross examination, the pancreas and jejunum in the SAP group appeared edematous at 24 h. The jejunum was full of yellow intestinal juice and ascites, and adhesions of organs were observed in 2 rats of the SAP group. Under light microscope examination, the pancreas from the S group exhibited no signs of pancreatitis (Figure 1A). Histological evaluation of the pancreas in rats with SAP revealed widespread acinar cell necrosis accompanied by edema, visible hemorrhage and inflammatory cell infiltrate (Figure 1B). In the S group, the structure of jejunum was normal (Figure 1C). In the SAP group, the mucosa was markedly denuded and partial loss of villous tissue with crypt layer infarction was also seen. Muscular layers showed slight alteration characterized by dilated thickness (Figure 1D).

Immunohistochemical staining

c-kit-positive cells could be divided into two cell populations. One population was mast cells situated within the mucosa layer (Figure 2A). The second population was ICC with large oval nuclei, sparse cytoplasm and branching processes; these cells were situated in the submuscular plexus (Figure 2B) and the intermuscular septa (Figure 2C). The density of c-kit-positive cells in the SAP group was significantly lower than in the S group; the respective mean densities were 88.47 ± 10.49 in the S group and 56.11 ± 7.09 in the SAP group.

Western blotting

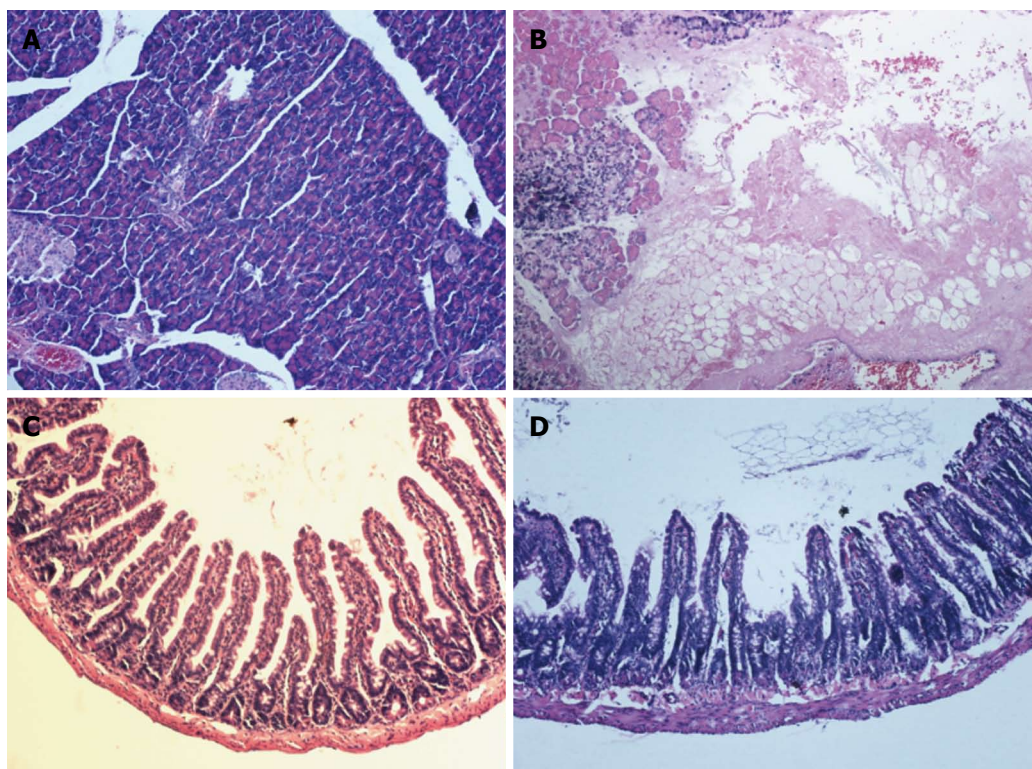Western blotting analysis using an antibody to c-kit on

Figure 1 Histological sections from pancreas and jejunum. A: The pancreas of the sham (S) group shows a normal exocrine and endocrine pancreatic architecture; B: The pancreas of severe acute pancreatitis (SAP) rats shows necrosis of the acinar cells accompanied by edema and hemorrhage; C: The structure of jejunum in the S group is normal; D: The mucosa was markedly denuded and the muscular layer was edematous in the SAP group. Magnification × 200.

tissue from the jejunum detected a protein band at approximately 145 kDa that corresponded to the molecular weight of c-kit protein (Figure 3A). The c-kit band density was clearly observed in the S group rats, but significantly reduced in comparison to the SAP group (relative protein expression: the S group, 0.53 ± 0.06; the SAP group, 0.36 ± 0.04, $P < 0.05$; Figure 3B). Consistent with immunohistochemical staining, lower levels of c-kit protein were demonstrated in the SAP group.

c-kit mRNA expression

Decreased expression of c-kit mRNA was demonstrated compared with the S group (Figure 4).

Ultrastructure of ICC

As previously described, ICC in control tissue are present in triangular or fusiform shapes. The nucleus of ICC is very voluminous surrounded by a small perinuclear cytoplasm that expands with long prolongations which are called cytoplasmic processes. The cytoplasm of these cells presents a higher electron density than the cytoplasm of the surrounding muscle cells. ICC contain mitochondria, rough and smooth endoplasmic reticulum, thin and intermediate filaments, caveolae, Golgi apparatus, free ribosomes and cytoplasmic vesicles. They are closely associated with smooth muscle and often network with other ICC. Some of them are intercalated between nerves and smooth muscle cells (Figure 5A-C).

In contrast with control tissues, confluent vacuoles were frequently present in ICC in tissue from the SAP group (Figure 5D). Mitochondria appeared damaged in some vacuolated processes (Figure 5E). Ultrastructural preservation of other cellular elements and organelles was mostly unaffected. Damage of the desmosome-like junctions between ICC and smooth muscle was also seen (Figure 5F).

DISCUSSION

SAP is a very common clinical disease and its mortality rate ranges from 10% in the case of sterile necrosis to 25% in the case of infected pancreatic necrosis[18,19]. Many studies have indicated that gastrointestinal dysmotility in rats with SAP could lead to the translocation of bacteria from the gut, thus resulting in pancreatic infections which have been suggested to be a major cause of death in SAP[20,21]. So it is very important to investigate the possible mechanisms of gastrointestinal dysmotility in SAP in order to reduce the mortality rate of SAP.

We used retrograde injection of 5% sodium taurocholate from the duodenal papilla to establish an SAP rat model. Pancreatic pathological changes, such as pancreatic hemorrhage, necrosis and infiltration of inflammatory cells, could be observed at 24 h after modeling. All these changes were consistent with patients with SAP. This demonstrated that the animal model of SAP was successfully established. In addition, a significantly decreased small intestine propulsion rate in rats with SAP was observed. Our results confirmed that experimental SAP induced intestinal motility disturbances as previously shown[22].
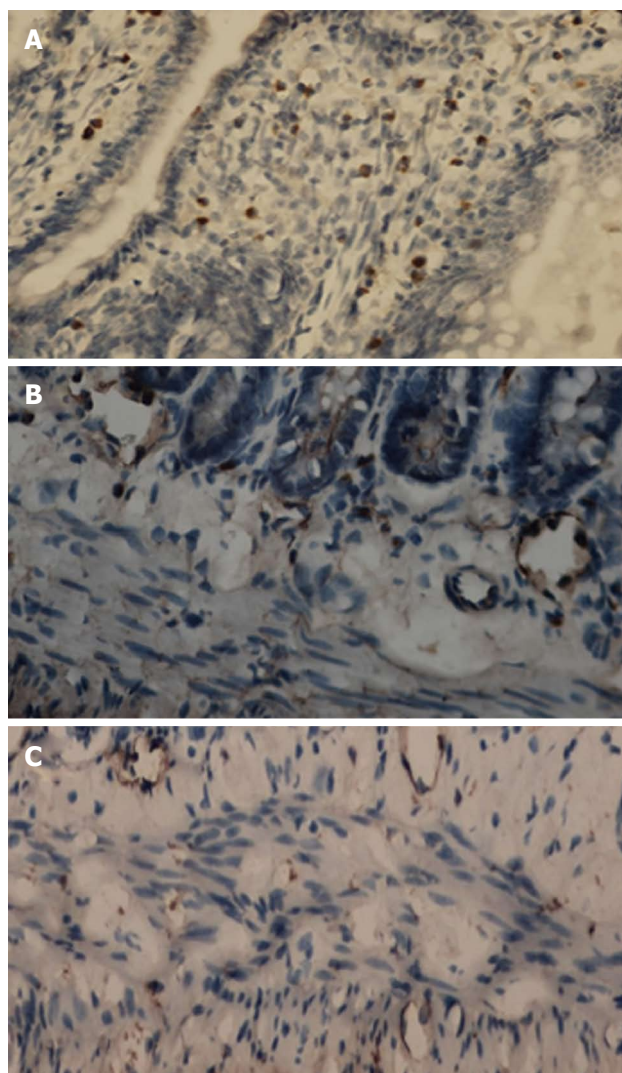
Figure 2 **Immunohistochemistry for c-kit.** A: Mucosal mast cells in rats retain c-kit positivity (internal control); B: c-kit-positive interstitial cells of Cajal (ICC) in the submuscular plexus in the sham group; C: c-kit-positive ICC in the intermuscular septa in the severe acute pancreatitis group. Magnification × 200.

Figure 3 **Expression of c-kit protein.** A: Bands of Western blotting of c-kit (145 kDa). β-actin is a loading control; B: Statistical analysis of relative density of Western blotting between two groups. Data are represented as mean ± SD. [a]*P* < 0.05 *vs* sham (S) group.

Figure 4 **Mean optical density of c-kit mRNA.** Each bar represents the mean ± SD (vertical line). [a]*P* < 0.05 *vs* sham (S) group. ICC: Interstitial cells of Cajal.

So far, the pathogenic mechanisms of pancreatitis-induced intestinal motility disturbances are largely unknown. It is well documented that ICC are implicated in the control of gastrointestinal motility. For example, decreased numbers or disrupted networks of ICC are associated with a number of human gastrointestinal motility disorders, including slow transit constipation[23,24], pseudo-obstruction[25-27] and diabetic enteropathy[28]. The potential role of ICC in the pathogenesis of gastrointestinal dysmotility in SAP has attracted attention. ICC can be classified into several subtypes according to their location in the gut wall; ICC at the level of the MY generates slow waves, and studies have confirmed that damage in the network of ICC-MY resulted in change of spontaneous mechanical contractions of the gut in a variety of human disease processes[29-31]. All these studies were focused on ICC-MY and spontaneous mechanical contractions. In addition to generating slow waves, other subsets of ICC ar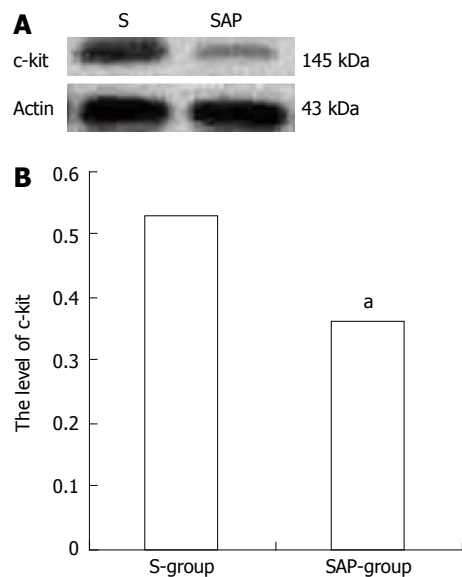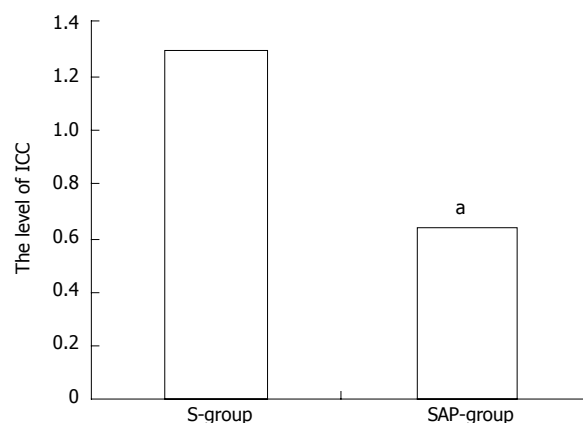e engaged in mediating enteric neural signals to the smooth muscles and acting as mechanosensors. In the present study, total ICC were observed by immunohistochemical staining. Around the submuscular plexus and in the intermuscular septa, we have demonstrated a decrease of c-kit-positive cells in these regions in the SAP group. Consistent with immunohistochemical staining, lower levels of c-kit protein were demonstrated in the SAP group.

Investigators have examined the ultrastructure of ICC by transmission electron microscopy in their intestinal obstruction model[30] and surgical resection model[31]. These findings all suggested that an actual change in ICC phenotype occurred from the ultrastructural appearance. Moreover, functionally mature ICC redifferentiated toward a smooth muscle cell phenotype when kit receptors were blocked[32]. Similarly, in our study, morphological changes such as vacuolation of mitochondria, irregular vacuoles and loosened desmosome-like junctions were
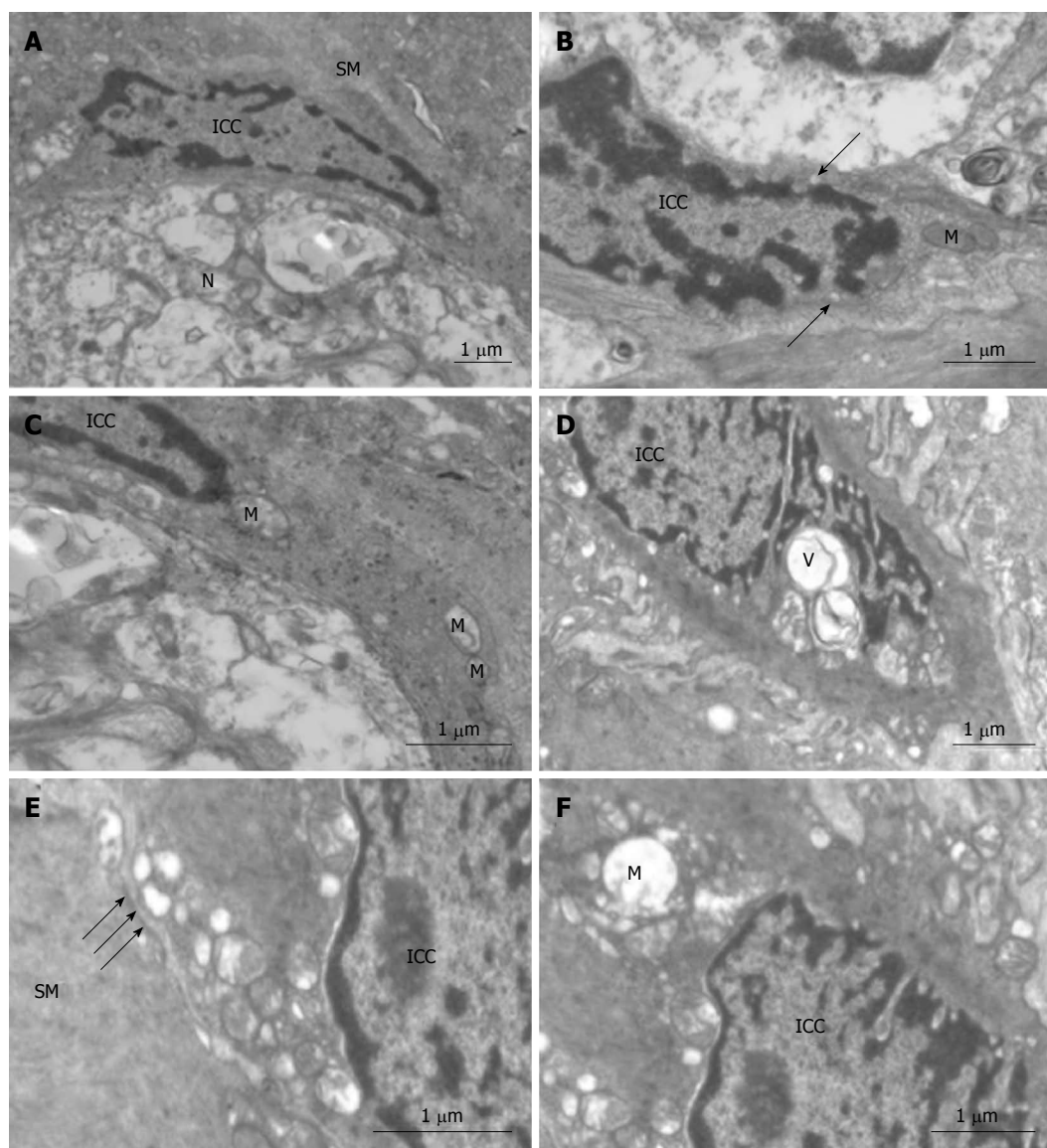
Figure 5 Ultrastructure of interstitial cells of Cajal. A-C: Control. A: Interstitial cells of Cajal (ICC) with fusiform nuclear morphology show an elongated nucleus with scarce perinuclear cytoplasm, and are situated between the smooth muscle (SM) and the enteric nerve (N). The cytoplasmic processes surround the external contours of the enteric nerve; B: Caveolae are lining cytoplasmic membrane (arrows); C: The processes of some ICC have characteristically numerous mitochondria (M); D-F: Severe acute pancreatitis. D: Vacuoles (V) are present in the ICC; E: The density of desmosome-like junction between ICC and smooth muscle is lower (arrows); F: Vacuolated mitochondria are present in the processes of ICC.

present in ICC in the SAP group, while the ultrastructure of ICC is normal in the S group. However, there is not sufficient evidence to support the theory that ICC transdifferentiate towards a smooth muscle cell phenotype. Although we did not investigate the amplitudes and frequencies of slow waves of the jejunum generated by ICC, it could be speculated that loss of ICC and changes of the ultrastructure influenced the function of ICC and eventually resulted in gastrointestinal dysmotility. The precise cellular changes that occur in response to the blockade of the c-kit signaling pathway are an extremely interesting direction for future investigation.

The present study further demonstrated that the expression of c-kit mRNA was significantly down-regulated in the SAP group. These data are consistent with previous reports that c-kit is down-regulated in the sigmoid colon

of patients with slow transit constipation[33] and in the gallbladders of guinea pigs on a high cholesterol diet[34]. In the gastrointestinal tract, development and maintenance of the ICC phenotype have been linked to intracellular signaling *via* c-kit. Beckett *et al*[35] have shown that blocking c-kit signaling during late gestation results in failure of ICC networks and pacemaker function to develop in the murine small intestine. Other investigators have shown that blockade of c-kit signaling caused redifferentiation of functionally mature ICC toward a smooth muscle cell phenotype[32]. In the present study, we provide additional evidence that the c-kit signaling pathway may be responsible for development and maintenance of the ICC. However, further studies are needed to demonstrate whether and when these changes could be restored to normal.

In conclusion, this study has disclosed that decreased

c-kit-positive cells and degenerative ultrastructural changes of ICC were present in the jejunum of rats with SAP, and that all these changes resulted from blockade of the c-kit signaling pathway. This study may provide new insights into pathological mechanisms of gastrointestinal motility disturbances in SAP. Since loss and proliferation of c-kit-positive cells lead to a variety of human gastrointestinal motility disorders[36-38] and gastrointestinal stromal tumors[39,40], thus developing the means to manipulate the ICC phenotype may have profound therapeutic benefits for these patients.

COMMENTS

Background
The incidence of intestinal dysmotility increases the mortality of patients with severe acute pancreatitis (SAP), but until now, the mechanism of this dysmotility is largely unknown. Many studies have reported that interstitial cells of Cajal (ICC), which are known as pacemaker cells, are associated with gastrointestinal dysmotility diseases.

Research frontiers
Loss and proliferation of ICC lead to a variety of human gastrointestinal motility disorders and gastrointestinal stromal tumors. However, the detailed changes of ICC in SAP are not clearly elucidated. In this study, the authors demonstrate that the loss and ultrastructural changes of ICC could be a potential mechanism for intestinal dysmotility in SAP.

Innovations and breakthroughs
Recent reports have highlighted the importance of ICC in gastrointestinal motility disorders and gastrointestinal stromal tumors. In gastrointestinal motility disorders, loss of ICC was present. This is the first study to report that loss of ICC was also present in SAP. Furthermore, the studies would suggest that the loss of ICC may result from blockade of the c-kit signaling pathway.

Applications
This study provided new insights into pathological mechanisms of gastrointestinal motility disturbances in SAP. Developing the means to manipulate the ICC may have profound therapeutic benefits.

Terminology
ICC were firstly described by the Spanish neuro-histologist Cajal. ICC are involved in processes such as generation of slow waves, neurotransmission and regulation of mechanical activities; all these processes are thought to be crucial in intestinal motility. SAP is a special type of acute pancreatitis accounting for 10% to 20% of all acute pancreatitis episodes; it is a dangerous condition with more complications and higher mortality.

Peer review
The authors examined the expression of c-kit and ultrastructural changes of ICC in jejunum in rats with experimental severe acute pancreatitis. The study revealed that decreased c-kit positive cells and degenerative ultrastructural changes of ICC were present; these changes were correlated to blockade of c-kit signaling pathway. The results are interesting and may provide new insights into pathological mechanisms of gastrointestinal dysmotility in SAP.

REFERENCES

1   **Sanders KM**. A case for interstitial cells of Cajal as pacemakers and mediators of neurotransmission in the gastrointestinal tract. *Gastroenterology* 1996; **111**: 492-515 [PMID: 8690216 DOI: 10.1053/gast.1996.v111.pm8690216]
2   **Sanders KM**, Ordög T, Koh SD, Torihashi S, Ward SM. Development and plasticity of interstitial cells of Cajal. *Neurogastroenterol Motil* 1999; **11**: 311-338 [PMID: 10520164 DOI: 10.1046/j.1365-2982.1999.00164.x]
3   **Takayama I**, Horiguchi K, Daigo Y, Mine T, Fujino MA, Ohno S. The interstitial cells of Cajal and a gastroenteric pacemaker system. *Arch Histol Cytol* 2002; **65**: 1-26 [PMID: 12002607 DOI: 10.1679/aohc.65.1]
4   **Sanders KM**, Ordög T, Ward SM. Physiology and pathophysiology of the interstitial cells of Cajal: from bench to bedside. IV. Genetic and animal models of GI motility disorders caused by loss of interstitial cells of Cajal. *Am J Physiol Gastrointest Liver Physiol* 2002; **282**: G747-G756 [PMID: 11960771]
5   **Hirst GD**, Ward SM. Interstitial cells: involvement in rhythmicity and neural control of gut smooth muscle. *J Physiol* 2003; **550**: 337-346 [PMID: 12794179 DOI: 10.1113/jphysiol.2003.043299]
6   **Huizinga JD**, Thuneberg L, Klüppel M, Malysz J, Mikkelsen HB, Bernstein A. W/kit gene required for interstitial cells of Cajal and for intestinal pacemaker activity. *Nature* 1995; **373**: 347-349 [PMID: 7530333]
7   **Burns AJ**, Herbert TM, Ward SM, Sanders KM. Interstitial cells of Cajal in the guinea-pig gastrointestinal tract as revealed by c-Kit immunohistochemistry. *Cell Tissue Res* 1997; **290**: 11-20 [PMID: 9377631 DOI: 10.1007/s004410050902]
8   **Hirota S**, Isozaki K, Nishida T, Kitamura Y. Effects of loss-of-function and gain-of-function mutations of c-kit on the gastrointestinal tract. *J Gastroenterol* 2000; **35** Suppl 12: 75-79 [PMID: 10779223]
9   **Kitamura Y**, Hirota S, Nishida T. A loss-of-function mutation of c-kit results in depletion of mast cells and interstitial cells of Cajal, while its gain-of-function mutation results in their oncogenesis. *Mutat Res* 2001; **477**: 165-171 [PMID: 11376697 DOI: 10.1016/S0027-5107(01)00117-8]
10   **Lecoin L**, Gabella G, Le Douarin N. Origin of the c-kit-positive interstitial cells in the avian bowel. *Development* 1996; **122**: 725-733 [PMID: 8631250]
11   **Rich A**, Miller SM, Gibbons SJ, Malysz J, Szurszewski JH, Farrugia G. Local presentation of Steel factor increases expression of c-kit immunoreactive interstitial cells of Cajal in culture. *Am J Physiol Gastrointest Liver Physiol* 2003; **284**: G313-G320 [PMID: 12388202]
12   **Zhou H**, Liu L, Bai Y, Wu W, Li G, Li J, Zou D, Gao J, Li Z. Damage of the interstitial cells of Cajal and myenteric neurons causing ileus in acute necrotizing pancreatitis rats. *Surgery* 2011; **149**: 262-275 [PMID: 20570303 DOI: 10.1016/j.surg.2010.04.023]
13   **Shimojima N**, Nakaki T, Morikawa Y, Hoshino K, Kitajima M. Imatinib blocks spontaneous mechanical activities in the adult mouse small intestine: possible inhibition of c-Kit signaling. *Pharmacology* 2005; **74**: 95-99 [PMID: 15722647 DOI: 10.1159/000084021]
14   **Wang X**, Gong Z, Wu K, Wang B, Yuang Y. Gastrointestinal dysmotility in patients with acute pancreatitis. *J Gastroenterol Hepatol* 2003; **18**: 57-62 [PMID: 12519225 DOI: 10.1046/j.1440-1746.2003.02898.x]
15   **Seerden TC**, De Man JG, Holzer P, Van den Bossche RM, Herman AG, Pelckmans PA, De Winter BY. Experimental pancreatitis disturbs gastrointestinal and colonic motility in mice: effect of the prokinetic agent tegaserod. *Neurogastroenterol Motil* 2007; **19**: 856-864 [PMID: 17883437 DOI: 10.1111/j.1365-2982.2007.00968.x]
16   **Leveau P**, Wang X, Soltesz V, Ihse I, Andersson R. Alterations in intestinal motility and microflora in experimental acute pancreatitis. *Int J Pancreatol* 1996; **20**: 119-125 [PMID: 8968867]
17   **Livak KJ**, Schmittgen TD. Analysis of relative gene expression data using real-time quantitative PCR and the 2(-Delta Delta C(T)) Method. *Methods* 2001; **25**: 402-408 [PMID: 11846609 DOI: 10.1006/meth.2001.1262]
18   **Swaroop VS**, Chari ST, Clain JE. Severe acute pancreatitis. *JAMA* 2004; **291**: 2865-2868 [PMID: 15199038 DOI: 10.1001/jama.291.23.2865]
19   **Dervenis C**, Johnson CD, Bassi C, Bradley E, Imrie CW, McMahon MJ, Modlin I. Diagnosis, objective assessment of severity, and management of acute pancreatitis. Santorini consensus conference. *Int J Pancreatol* 1999; **25**: 195-210 [PMID:

10453421]

20   **Van Felius ID**, Akkermans LM, Bosscha K, Verheem A, Harmsen W, Visser MR, Gooszen HG. Interdigestive small bowel motility and duodenal bacterial overgrowth in experimental acute pancreatitis. *Neurogastroenterol Motil* 2003; **15**: 267-276 [PMID: 12787336 DOI: 10.1046/j.1365-2982.2003.00410.x]

21   **Beger HG**, Bittner R, Block S, Büchler M. Bacterial contamination of pancreatic necrosis. A prospective clinical study. *Gastroenterology* 1986; **91**: 433-438 [PMID: 3522342]

22   **Chen X**, Valente JF, Alexander JW. The effect of sennosides on bacterial translocation and survival in a model of acute hemorrhagic pancreatitis. *Pancreas* 1999; **18**: 39-46 [PMID: 9888659 DOI: 10.1097/00006676-199901000-00006]

23   **He CL**, Burgart L, Wang L, Pemberton J, Young-Fadok T, Szurszewski J, Farrugia G. Decreased interstitial cell of cajal volume in patients with slow-transit constipation. *Gastroenterology* 2000; **118**: 14-21 [PMID: 10611149 DOI: 10.1016/S0016-5085(00)70409-4]

24   **Lyford GL**, He CL, Soffer E, Hull TL, Strong SA, Senagore AJ, Burgart LJ, Young-Fadok T, Szurszewski JH, Farrugia G. Pan-colonic decrease in interstitial cells of Cajal in patients with slow transit constipation. *Gut* 2002; **51**: 496-501 [PMID: 12235070 DOI: 10.1016/S0016-5085(00)85604-8]

25   **Kenny SE**, Vanderwinden JM, Rintala RJ, Connell MG, Lloyd DA, Vanderhaegen JJ, De Laet MH. Delayed maturation of the interstitial cells of Cajal: a new diagnosis for transient neonatal pseudoobstruction. Report of two cases. *J Pediatr Surg* 1998; **33**: 94-98 [PMID: 9473109 DOI: 10.1016/S0022-3468(98)90370-0]

26   **Vanderwinden JM**, Rumessen JJ. Interstitial cells of Cajal in human gut and gastrointestinal disease. *Microsc Res Tech* 1999; **47**: 344-360 [PMID: 10602294 DOI: 10.1002/(SICI)1097-0029(19991201)47:]

27   **Feldstein AE**, Miller SM, El-Youssef M, Rodeberg D, Lindor NM, Burgart LJ, Szurszewski JH, Farrugia G. Chronic intestinal pseudoobstruction associated with altered interstitial cells of cajal networks. *J Pediatr Gastroenterol Nutr* 2003; **36**: 492-497 [PMID: 12658043 DOI: 10.1097/00005176-200304000-00016]

28   **He CL**, Soffer EE, Ferris CD, Walsh RM, Szurszewski JH, Farrugia G. Loss of interstitial cells of cajal and inhibitory innervation in insulin-dependent diabetes. *Gastroenterology* 2001; **121**: 427-434 [PMID: 11487552 DOI: 10.1053/gast.2001.26264]

29   **Shimojima N**, Nakaki T, Morikawa Y, Hoshino K, Ozaki H, Hori M, Kitajima M. Interstitial cells of Cajal in dysmotility in intestinal ischemia and reperfusion injury in rats. *J Surg Res* 2006; **135**: 255-261 [PMID: 16872634 DOI: 10.1016/j.jss.2006.04.022]

30   **Chang IY**, Glasgow NJ, Takayama I, Horiguchi K, Sanders KM, Ward SM. Loss of interstitial cells of Cajal and development of electrical dysfunction in murine small bowel obstruction. *J Physiol* 2001; **536**: 555-568 [PMID: 11600689 DOI: 10.1111/j.1469-7793.2001.0555c.xd]

31   **Yanagida H**, Yanase H, Sanders KM, Ward SM. Intestinal surgical resection disrupts electrical rhythmicity, neural responses, and interstitial cell networks. *Gastroenterology* 2004; **127**: 1748-1759 [PMID: 15578513 DOI: 10.1053/j.gastro.2004.09.053]

32   **Torihashi S**, Nishi K, Tokutomi Y, Nishi T, Ward S, Sanders KM. Blockade of kit signaling induces transdifferentiation of interstitial cells of cajal to a smooth muscle phenotype. *Gastroenterology* 1999; **117**: 140-148 [PMID: 10381920 DOI: 10.1016/S0016-5085(99)70560-3]

33   **Tong WD**, Liu BH, Zhang LY, Xiong RP, Liu P, Zhang SB. Expression of c-kit messenger ribonucleic acid and c-kit protein in sigmoid colon of patients with slow transit constipation. *Int J Colorectal Dis* 2005; **20**: 363-367 [PMID: 15688149 DOI: 10.1007/s00384-004-0679-0]

34   **Hu WM**, Luo HS, Ding XW, Wang L. Expression of C-kit messenger ribonucleic acid and C-kit protein in the gallbladders in guinea pigs of high cholesterol diet. *Dig Dis Sci* 2009; **54**: 1651-1655 [PMID: 18987972 DOI: 10.1007/s10620-008-0552-z]

35   **Beckett EA**, Ro S, Bayguinov Y, Sanders KM, Ward SM. Kit signaling is essential for development and maintenance of interstitial cells of Cajal and electrical rhythmicity in the embryonic gastrointestinal tract. *Dev Dyn* 2007; **236**: 60-72 [PMID: 16937373 DOI: 10.1002/dvdy.20929]

36   **Sanders KM**, Koh SD, Ward SM. Organization and electrophysiology of interstitial cells of Cajal and smooth muscle cells in the gastrointestinal tract. 4th ed. Johnson LR, editor. Physiology of the gastrointestinal tract: Elsevier Press, 2006: 533-576 [DOI: 10.1016/B978-012088394-3/50023-4]

37   **Rolle U**, Piasecna-Piotrowska A, Puri P. Interstitial cells of Cajal in the normal gut and in intestinal motility disorders of childhood. *Pediatr Surg Int* 2007; **23**: 1139-1152 [PMID: 17968564 DOI: 10.1007/s00383-007-2022-7]

38   **Midrio P**, Vannucchi MG, Pieri L, Alaggio R, Faussone-Pellegrini MS. Delayed development of interstitial cells of Cajal in the ileum of a human case of gastroschisis. *J Cell Mol Med* 2008; **12**: 471-478 [PMID: 18266958 DOI: 10.1111/j.1582-4934.2008.00277.x]

39   **Hirota S**, Isozaki K, Moriyama Y, Hashimoto K, Nishida T, Ishiguro S, Kawano K, Hanada M, Kurata A, Takeda M, Muhammad Tunio G, Matsuzawa Y, Kanakura Y, Shinomura Y, Kitamura Y. Gain-of-function mutations of c-kit in human gastrointestinal stromal tumors. *Science* 1998; **279**: 577-580 [PMID: 9438854 DOI: 10.1126/science.279.5350.577]

40   **Nishida T**, Hirota S, Taniguchi M, Hashimoto K, Isozaki K, Nakamura H, Kanakura Y, Tanaka T, Takabayashi A, Matsuda H, Kitamura Y. Familial gastrointestinal stromal tumours with germline mutation of the KIT gene. *Nat Genet* 1998; **19**: 323-324 [PMID: 9697690]